Arch. Pharm. Chem. Life Sci. 2016, *349*, 356–362

ARCH PHARM
Archiv der Pharmazie

Full Paper

Discovery of 4-(Piperazin-1-yl)-7*H*-pyrrolo[2,3-d]pyrimidine Derivatives as Akt Inhibitors

Yang Liu[1], Yanzhen Yin[1], Jingya Zhang[1], Krystle Nomie[2], Liang Zhang[2], Dezhi Yang[1], Michael L. Wang[2], and Guisen Zhao[1]*

[1] Department of Medicinal Chemistry, Key Laboratory of Chemical Biology (Ministry of Education), School of Pharmaceutical Sciences, Shandong University, Jinan, Shandong, P. R. China
[2] The University of Texas MD Anderson Cancer Center, Houston, TX, USA

A series of 4-(piperazin-1-yl)-7*H*-pyrrolo[2,3-d]pyrimidine derivatives was synthesized and evaluated as Akt inhibitors by optimization of a weak screening lead (**1**). Typically, compounds **5q** and **5t** significantly improved the Akt1 inhibitory potency with IC_{50} values of 18.0 and 21.3 nM, respectively, with desirable antiproliferative effect against the cell lines LNCaP and PC-3. The inhibitors **5q** and **5t** might serve as lead compounds for further exploration of Akt inhibitors as anticancer agents.

Keywords: Akt / Anticancer / Docking / Pyrrolopyrimidines

Received: November 27, 2015; Revised: February 23, 2016; Accepted: February 25, 2016

DOI 10.1002/ardp.201500427

Additional supporting information may be found in the online version of this article at the publisher's web-site.

Introduction

The phosphoinositide 3-kinase (PI3K)/Akt signaling pathway is an important signal transduction pathway that regulates multiple cellular processes, including cell proliferation, transformation, and differentiation [1]. Akt, also known as protein kinase B (PKB), is a serine/threonine kinase that functions as a critical junction in the PI3K-Akt signaling cascade. To date, three closely related Akt isoforms have been identified: Akt1 (PKBα), Akt2 (PKBβ), and Akt3 (PKBγ) [2]. All of these homologous isoforms have 97–100% sequence identity in the ATP-binding site and share a common structural organization comprising three functional domains: the N-terminal pleckstrin homology (PH) domain, the central catalytic domain, and the C-terminal regulatory domain [3].

As a pivotal node in the PI3K/Akt pathway, when dually phosphorylated by 3-phosphoinositide-dependent protein kinase 1 (PDK1) at Thr^{308} and by mammalian target of rapamycin complex 2 (mTORC2) at Ser^{473}, Akt phosphorylates a wide range of effectors that regulate tumor-associated cell survival and proliferation [4]. These effectors, including glycogen synthase kinase 3 (GSK-3), proapoptotic proteins Bad and BAX, tuberous sclerosis protein complex 1/2 (TSC1/2) and others, block apoptosis and maintain the proliferation of tumor cells when phosphorylated [5]. Ectopic expression of constitutively active Akt has been observed in many cancers such as breast cancer [6], ovarian carcinoma [7], and prostate cancer [8]. Furthermore, aberrant activation of Akt renders tumor cells resistant to chemotherapeutic drugs such as monoclonal antibodies [9]. Overall, these findings suggest that Akt is a well-validated target for anticancer drug discovery.

Significant efforts have been made to explore Akt inhibitors [10]. A self-established compounds library comprising different structural scaffolds has been established for random screening of anticancer candidates, in which the novel pyrrolopyrimidine-based lead **1** was discovered to exhibit inhibitory activity against Akt1 with an inhibition

Correspondence: Prof. Guisen Zhao, Department of Medicinal Chemistry, School of Pharmaceutical Sciences, Shandong University, Jinan, Shandong 250012, P. R. China.
E-mail: guisenzhao@sdu.edu.cn
Fax: +86-531-88382009

*Additional correspondence: Prof. Michael L. Wang,
E-mail: wang@mdanderson.org

rate of 70.1% at 5 μM, making compound **1** the potential lead compound for further exploration of Akt inhibitors. Herein we describe the structural modifications of compound **1**, with halogen atoms at the 5-position on the pyrrolopyrimidine core and substituted phenyls or naphthyls linked to the 4-piperazine moiety through an acetamide bond, which led to a series of 4-(piperazin-1-yl)-7*H*-pyrrolo[2,3-d]pyrimidine derivatives evaluated as Akt inhibitors (Fig. 1).

Results and discussion

Chemistry

The synthesis of the pyrrolopyrimidine derivatives is depicted in Scheme 1. Briefly, treatment of the readily available 4-chloro-7*H*-pyrrolo[2,3-d]pyrimidine (**2a**) with *N*-chlorosuccinimide (NCS) or *N*-bromosuccinimide (NBS) caused clean chlorination or bromination at C5 to give 4,5-dichloro-7*H*-pyrrolo[2,3-d]pyrimidine (**2b**) or 5-bromo-4-chloro-7*H*-pyrrolo[2,3-d]pyrimidine (**2c**), respectively. Subsequent incorporation of the Boc-protected piperazine via aromatic nucleophilic substitution delivered **3a–c**. Acid-promoted Boc deprotection provided key intermediates **4a–c** as dihydrochloride salts. Finally, the designed 4-(piperazin-1-yl)-7*H*-pyrrolo[2,3-d]pyrimidine derivatives (**5a–u**) were achieved by amide coupling with the requisite cores **4** and commercially available substituted acetic acids.

Biology

Twenty-one 4-(piperazin-1-yl)-7*H*-pyrrolo[2,3-d]pyrimidine derivatives were prepared. Their Akt1 inhibitory activities were detected using a homogeneous time-resolved fluorescence (HTRF) kinase activity assay, the inhibition ratios were determined at dual concentrations of 50 nM and 5 μM, respectively (Table 1).

As depicted in Table 1, most of the synthesized compounds showed over-half inhibition potency at 5 μM against Akt1. Considering the enzyme inhibitory activity at 50 nM, almost no Akt1 inhibitory activity was observed for C5 hydrogen analogs (**5a–j**). Introduction of a chlorine or bromine atom at C5 on the pyrrolopyrimidine core produced potent enzyme inhibition (**5l**, **5p** vs. **5e**). Insight into the R_2 substitution, unsubstituted phenyl compound **5n** or replacement of the phenyl ring with a naphthyl moiety (**5u**) resulted in significantly decreased potency versus Akt1. Furthermore, the addition of *para*-substituents of the phenyl group yielded an improved potency in Akt1 inhibition than *meta*-substituents (**5k** vs. **5l**, **5o** vs. **5p**). The *para*-chloro/bromo-phenyl (**5l**, **5p**, and **5q**) and the 3,4-dichloro substitution (**5t**) is essential for Akt1 inhibitory potency, methoxyl substitution (**5r**) led to moderately decreased Akt1 inhibitory activity, while the *tert*-butyl derivative (**5s**) led to a substantial reduction in Akt1 potency by more than 10-fold.

Compounds with over-half inhibition at 50 nM were further selectively investigated for their IC_{50} values against Akt1 and cellular potency against the LNCaP and PC-3 cell lines. As shown in Table 2, in comparison with compound **1**, compounds **5l**, **5p**, **5q**, and **5t** significantly improved the enzyme inhibitory potency and antiproliferative activity against LNCaP and PC-3 cell lines, indicating that these compounds blocked proliferation in prostate cancer cells partly through inhibiting Akt activity. Notably, the most potent compound **5q** inhibited Akt1 with an IC_{50} value of 18.0 nM, and the 3,4-dichloro substitution (**5t**) exhibited comparable potency (IC_{50} = 21.3 nM).

Molecular modeling

Compound **5q** was chosen for molecular modeling to rationalize the observed activity against Akt1 (PDB: 4EKL) using Sybyl 1.1 software package. As depicted in Fig. 2, compound **5q** nicely occupied the ATP cleft, the *para*-chlorophenyl group entered the hydrophobic pocket B formed by Gly159, Phe161, Gly162, and Leu181. The pyrrolopyrimidine core formed a pair of key hydrogen bonds to residues Ala230 and Glu228 in pocket A. Though no obvious interaction between the bromine atom and the protein was observed, the C-5 bromine substitution, with improved size and hydrophobicity, was in proximity to the lipophilic side chains of Ala177, Val164, and Met227, which might be responsible for the improved potency.

Conclusion

In summary, optimization of the pyrrolopyrimidine lead compound **1** as novel Akt1 inhibitors was performed. Among the synthesized compounds, compounds **5q** and **5t** inhibited Akt1 kinase activity with IC_{50} values of 18.0 and 21.3 nM, respectively, and displayed desirable antiproliferative effect against LNCaP and PC-3 cell lines with IC_{50} values at low micromolar level. Structure–activity relationship analysis revealed that the chloro- or bromo-substitution at the 5-position of the pyrrolopyrimidine core and the 4-Cl/3,4-diCl-substituted phenyl moiety linked to piperazine ring is critical to the enzyme inhibitory activity and cell potency. The compounds **5q** and **5t** might serve as lead compounds for further exploration of Akt inhibitors as anticancer agents.

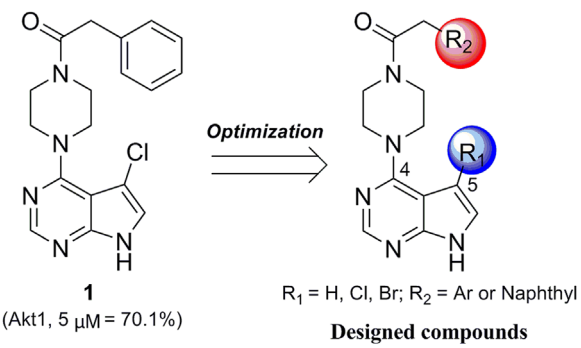

Figure 1. Structures of the lead **1** and designed compounds.

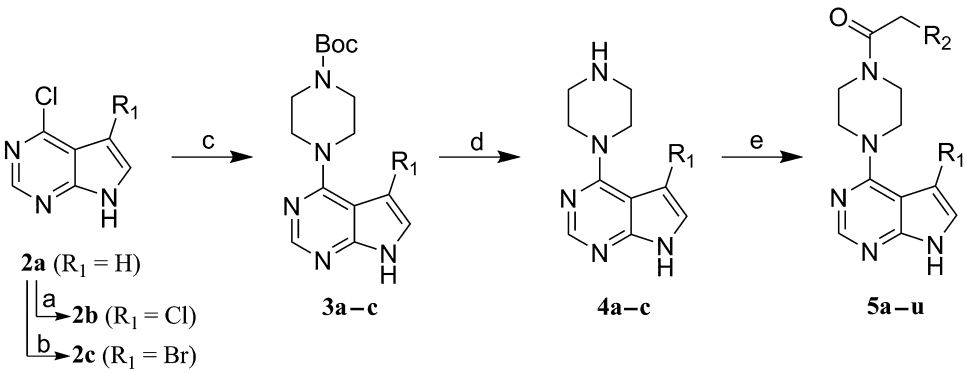

R_2 = Ph; 3-Br-Ph; 4-Br-Ph; 4-Cl-Ph; 4-F-Ph, 4-OCH_3-Ph; 4-tBu-Ph; 3,4-diCl-Ph; 2,4-diCl-Ph; Naphth-1-yl; Naphth-2-yl.

Scheme 1. Synthesis of compounds **5a–u**. Reagents and conditions: (a) NCS, DMF, rt, 72 h; (b) NBS, DMF, rt, 72 h; (c) *N*-Boc-piperazine, DMF, 110°C, 16 h; (d) 4 M HCl in dioxane, CH_3OH, rt, 24 h; (e) substituted acetic acid, EDCI, HOBT, DIEA, THF, rt, 24 h.

Experimental

Chemistry

All of the materials were obtained from commercial suppliers and used without further purification. All reactions were monitored by thin layer chromatography (TLC), and silica gel GF254 plates were used and visualized with UV light. Column chromatography was performed with silica gel using the indicated solvents. ^{1}H NMR and ^{13}C NMR spectra were recorded on a Varian Inova 600 (Switzerland) or Bruker

Table 1. The inhibitory effects of pyrrolopyrimidine derivatives on Akt1 activity.

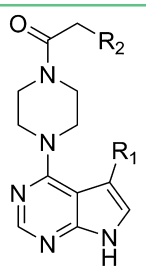

Code	R_1	R_2	Inhibition of Akt1 activity (%)		Code	R_1	R_2	Inhibition of Akt1 activity (%)	
			50 nM	5 μM				50 nM	5 μM
5a	H	Ph	9.2	34.3	**5l**	Cl	4-Br-Ph	71.5	99.8
5b	H	3-Br-Ph	5.0	80.5	**5m**	Cl	naphth-2-yl	14.3	95.0
5c	H	4-F-Ph	NA	88.9	**5n**	Br	Ph	NA	88.3
5d	H	4-Cl-Ph	12.4	99.4	**5o**	Br	3-Br-Ph	18.7	98.5
5e	H	4-Br-Ph	16.0	98.5	**5p**	Br	4-Br-Ph	69.5	100.0
5f	H	4-tBu-Ph	NA	39.3	**5q**	Br	4-Cl-Ph	69.7	96.6
5g	H	4-CH_3O-Ph	NA	76.1	**5r**	Br	4-CH_3O-Ph	36.6	99.2
5h	H	2,4-diCl-Ph	NA	66.2	**5s**	Br	4-tBu-Ph	5.3	82.4
5i	H	naphth-1-yl	5.2	29.4	**5t**	Br	3,4-diCl-Ph	65.5	100.0
5j	H	naphth-2-yl	8.3	92.4	**5u**	Br	naphth-2-yl	NA	97.0
5k	Cl	3-Br-Ph	15.0	98.1	**1**	Cl	Ph	NA	70.1

NA, not active.

Table 2. The inhibitory effects of pyrrolopyrimidine derivatives on Akt1 activity and prostate cancer cells.

Code	Akt1, IC_{50}[a)] (nM)	LNCaP, IC_{50}[a)] (μM)	PC-3, IC_{50}[a)] (μM)
5l	45.3 ± 0.6	6.6 ± 2.0	25.3 ± 1.3
5p	31.6 ± 2.2	9.8 ± 1.1	38.7 ± 0.6
5q	18.0 ± 0.7	9.3 ± 1.9	21.1 ± 1.6
5t	21.3 ± 1.4	7.0 ± 0.5	31.5 ± 0.2
1	>1000	45.0 ± 0.9	70.4 ± 1.5

[a)] IC_{50} data are the mean of three independent measurements.

Avance III 400 (Germany) spectrometer using TMS as an internal standard in DMSO-d_6. Chemical shifts are reported in parts per million (ppm). Coupling constants (*J*) are given in Hertz. The mass spectra (MS) were measured with an API 4000. All of the melting points were determined on a capillary melting point apparatus RY-1G (TianGuang Optical Instruments, Inc., China) and are uncorrected. Human Akt1 was obtained from Carna Biosciences, Inc. (Canada) and the HTRF assay kit was purchased from Cisbio Bioassays, Inc. (France).

Please see the Supporting Information for the InChI codes of the new compounds.

General methods for preparation of the compounds

*Preparation of **2b,c***

To a solution of **2a** (3.0 g, 20 mmol) in *N*,*N*-dimethylformamide (DMF) (30 mL) was added NCS/NBS (21 mmol). The mixture was stirred at room temperature for 72 h. The mixture was poured into ice water (300 mL) and the precipitate was filtered, washed with water (3 × 10 mL), and dried to obtain **2b**,**c**.

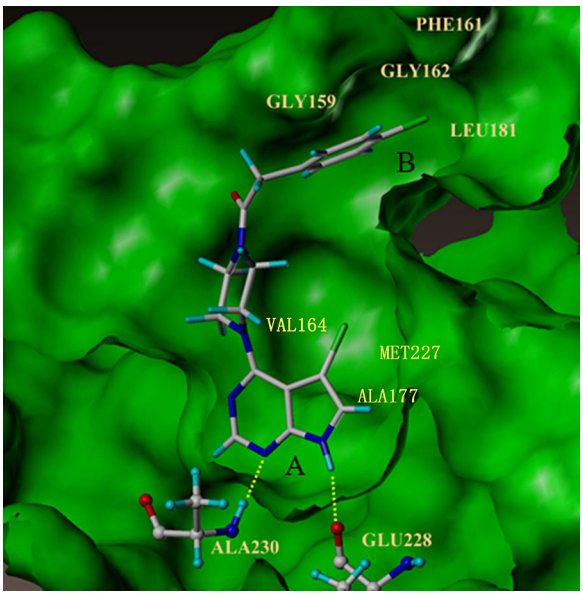

Figure 2. The predicted binding mode of **5q** at the ATP-binding site of Akt1.

*4,5-Dichloro-7H-pyrrolo[2,3-d]pyrimidine (**2b**)*

Gray powder, yield 95%, mp: 287–290°C, ^{1}H NMR (400 MHz, DMSO) δ (ppm): 12.87 (s, 1H), 8.63 (s, 1H), 7.91 (s, 1H). MS (ESI) *m/z*: 188 $[M+H]^+$.

*5-Bromo-4-chloro-7H-pyrrolo[2,3-d]pyrimidine (**2c**)*

Pale powder, yield 95%, mp: 290–292°C, ^{1}H NMR (400 MHz, DMSO) δ (ppm): 13.00 (s, 1H), 8.64 (s, 1H), 7.97 (s, 1H). MS (ESI) *m/z*: 232 $[M+H]^+$.

*Preparation of **3a–c***

To a solution of **2a–c** (3.2 mmol) in DMF (3 mL) were added *N*-Boc-piperazine (3.6 mmol, 750 mg) and triethylamine (Et_3N) (4.9 mmol, 0.65 mL). The reaction mixture was heated for 16 h at 110°C, then treated with water (300 mL) and extracted with ethyl acetate (EtOAc) (4 × 60 mL). The combined organic phases were washed with brine (2 × 50 mL), dried over sodium sulfate (Na_2SO_4), filtered and concentrated *in vacuo*. The crude residue was purified by column chromatography with petroleum ether/ethyl acetate (1:3) to obtain **3a–c**.

*Tert-butyl-4-(7H-pyrrolo[2,3-d]pyrimidin-4-yl)piperazine-1-carboxylate (**3a**)*

Offwhite solid, yield 59%, ^{1}H NMR (600 MHz, DMSO) δ (ppm): 11.73 (s, 1H), 8.15 (s, 1H), 7.20 (d, *J* = 0.6 Hz, 1H), 6.64 (d, *J* = 1.8 Hz, 1H), 3.86 (s, 4H), 3.48 (s, 4H), 1.43 (s, 9H). MS (ESI) *m/z*: 304 $[M+H]^+$.

*Tert-butyl 4-(5-chloro-7H-pyrrolo[2,3-d]pyrimidin-4-yl)-piperazine-1-carboxylate (**3b**)*

Offwhite solid, yield: 51%. ^{1}H NMR (400 MHz, DMSO) δ (ppm): 12.23 (s, 1H), 8.29 (s, 1H), 7.52 (d, *J* = 2.8 Hz, 1H), 3.52 (s, 8H), 1.42 (s, 9H). MS (ESI) *m/z*: 338 $[M+H]^+$.

*Tert-butyl 4-(5-bromo-7H-pyrrolo[2,3-d]pyrimidin-4-yl)-piperazine-1-carboxylate (**3c**)*

Pale yellow solid, yield 48%, ^{1}H NMR (400 MHz, DMSO) δ (ppm): 12.21 (s, 1H), 8.37 (s, 1H), 7.52 (d, *J* = 2.6 Hz, 1H), 3.52 (s, 8H), 1.42 (s, 9H). MS (ESI) *m/z*: 382 $[M+H]^+$.

*Preparation of **4a–c***

To 4 M HCl in dioxane (5 mL) was added **3a–c** (1 mmol). The reaction mixture was stirred for 24 h at room temperature. The precipitate was isolated by filtration, washed with diethyl

ARCH PHARM
Archiv der Pharmazie

ether (2 × 5 mL), and dried to obtain **4a–c**, which was used for the next step without further purification.

*Preparation of **5a–u***

To a solution of substituted acetic acids (0.365 mmol) in dry tetrahydrofuran (THF) (6 mL) at 0°C were added 1-(3-dimethylaminopropyl)-3-ethylcarbodiimide hydrochloride (EDCI) (77 mg, 0.4 mmol), 1-hydroxybenzotriazole (HOBt) (61 mg, 0.4 mmol) and *N*,*N*-diisopropylethylamine (DIEA) (141 mg, 1.1 mmol). The reaction mixture was stirred for 30 min before **4a–c** (0.365 mmol) was added portionwise. Then the reaction was warmed to room temperature and stirred for another 24 h. The mixture was diluted with ethyl acetate (20 mL) and washed with sodium bicarbonate solution (10%, 20 mL), water (20 mL), and brine (20 mL). The organic layer was dried over Na_2SO_4, filtered, and concentrated *in vacuo*. The crude residue was purified by recrystallization using petroleum ether/ethyl acetate to obtain **5a–u**.

*1-(4-(7H-Pyrrolo[2,3-d]pyrimidin-4-yl)piperazin-1-yl)-2-phenylethanone (**5a**)*

White solid, yield 80%, purity 98.2%, mp: 169–172°C, ^{1}H NMR (400 MHz, DMSO) δ (ppm): 11.71 (s, 1H), 8.15 (s, 1H), 7.33–7.19 (m, 6H), 6.61 (t, J = 1.6 Hz, 1H), 3.87–3.83 (m, 4H), 3.77 (s, 2H), 3.68–3.64 (m, 4H). ^{13}C NMR (100 MHz, DMSO) δ (ppm): 169.6, 156.8, 152.4, 150.9, 136.2, 129.5 (2C), 128.7 (2C), 126.8, 122.0, 102.8, 101.2, 45.3 (2C), 45.3 (2C), 41.5. MS (ESI) *m/z*: 322 $[M+H]^+$.

*1-(4-(7H-Pyrrolo[2,3-d]pyrimidin-4-yl)piperazin-1-yl)-2-(3-bromophenyl)ethanone (**5b**)*

White solid, yield 89%, purity 97.1%, mp: 150–152°C, ^{1}H NMR (400 MHz, DMSO) δ (ppm): 8.16 (s, 1H), 7.47–7.43 (m, 2H), 7.30–7.26 (m, 2H), 7.21 (s, 1H), 6.63 (s, 1H), 3.88 (s, 4H), 3.80 (s, 2H), 3.69–3.60 (m, 4H). ^{13}C NMR (100 MHz, DMSO) δ (ppm): 169.2, 156.8, 152.4, 151.0, 139.1, 132.6, 130.7, 129.7, 128.9, 122.0, 121.8, 102.8, 101.2, 45.3 (4C), 41.5. MS (ESI) *m/z*: 400 $[M+H]^+$.

*1-(4-(7H-Pyrrolo[2,3-d]pyrimidin-4-yl)piperazin-1-yl)-2-(4-fluorophenyl)ethanone (**5c**)*

Pale yellow solid, yield 81%, purity 97.8%, mp: 194–197°C, ^{1}H NMR (400 MHz, DMSO) δ (ppm): 11.67 (s, 1H), 8.16 (s, 1H), 7.28 (m, 2H), 7.21–7.17 (m, 1H), 7.14–7.10 (m, 2H), 6.61 (dd, J_1 = 3.4 Hz, J_2 = 1.7 Hz, 1H), 3.86 (d, J = 5.2 Hz, 4H), 3.76 (s, 2H), 3.69–3.62 (m, 4H). ^{13}C NMR (100 MHz, DMSO) δ (ppm): 169.3, 159.6, 152.1, 151.1, 135.4, 131.9, 131.5 (2C), 129.1, 128.6 (2C), 124.8, 104.9, 50.4 (2C), 50.2 (2C), 41.6. MS (ESI) *m/z*: 340 $[M+H]^+$.

*1-(4-(7H-Pyrrolo[2,3-d]pyrimidin-4-yl)piperazin-1-yl)-2-(4-chlorophenyl)ethanone (**5d**)*

White solid, yield 87%, purity 98.2%, mp: 175–178°C, ^{1}H NMR (400 MHz, DMSO) δ (ppm): 11.72 (s, 1H), 8.15 (s, 1H), 7.36 (d, J = 8.36 Hz, 2H), 7.27 (d, J = 8.36 Hz, 2H), 6.61 (dd, J_1 = 3.32 Hz, J_2 = 1.68 Hz, 1H), 3.87 (t, J = 4.64 Hz, 4H), 3.78 (s, 2H), 3.69–3.64 (m, 4H). ^{13}C NMR (100 MHz, DMSO) δ (ppm): 169.3, 156.8, 152.4, 150.9, 135.3, 131.6 (2C), 131.5, 128.6 (2C), 122.0, 102.8, 101.2, 45.3 (4C), 41.5. MS (ESI) *m/z*: 356 $[M+H]^+$.

*1-(4-(7H-Pyrrolo[2,3-d]pyrimidin-4-yl)piperazin-1-yl)-2-(4-bromophenyl)ethanone (**5e**)*

Pale yellow solid, yield 75%, purity 98.5%, mp: 175–177°C, ^{1}H NMR (400 MHz, DMSO) δ (ppm): 11.73 (s, 1H), 8.16 (s, 1H), 7.50 (d, J = 8.4 Hz, 2H), 7.21 (d, J = 8.4 Hz, 3H), 6.62 (s, 1H), 3.92–3.82 (m, 4H), 3.77 (s, 2H), 3.72–3.59 (m, 4H). ^{13}C NMR (100 MHz, DMSO) δ (ppm): 169.5, 156.8, 152.4, 150.9, 131.5, 131.4, 122.0, 115.5 (2C), 115.3 (2C), 102.8, 101.2, 45.3 (4C), 41.5. MS (ESI) *m/z*: 400 $[M+H]^+$.

*1-(4-(7H-Pyrrolo[2,3-d]pyrimidin-4-yl)piperazin-1-yl)-2-(4-(tert-butyl)phenyl)ethanone (**5f**)*

White solid, yield 82%, purity 96.2%, mp: 222–225°C, ^{1}H NMR (400 MHz, DMSO) δ (ppm): 11.74 (s, 1H), 8.15 (s, 1H), 7.33 (d, J = 12 Hz, 2H), 7.20–7.16 (m, 3H), 6.61 (s, 1H), 3.85 (s, 4H), 3.72 (s, 2H), 3.65 (d, J = 12 Hz, 4H), 1.26 (s, 9H). ^{13}C NMR (100 MHz, DMSO) δ (ppm): 169.8, 156.8, 152.4, 150.9, 149.1, 133.1, 129.1 (2C), 125.5 (2C), 122.0, 102.8, 101.2, 46.1 (4C), 41.5, 34.5, 31.6 (3C). MS (ESI) *m/z*: 378 $[M+H]^+$.

*1-(4-(7H-Pyrrolo[2,3-d]pyrimidin-4-yl)piperazin-1-yl)-2-(4-methoxyphenyl)ethanone (**5g**)*

Yellow solid, yield 87%, purity 97.3%, mp: 170–174°C, ^{1}H NMR (400 MHz, DMSO) δ (ppm): 11.74 (s, 1H), 8.15 (s, 1H), 7.20–7.16 (m, 3H), 6.87 (d, J = 8.4 Hz, 2H), 6.61 (s, 1H), 3.85–3.82 (m, 4H), 3.72 (s, 3H), 3.69 (s, 2H), 3.64 (s, 4H). ^{13}C NMR (100 MHz, DMSO) δ (ppm): 169.9, 158.3, 156.8, 152.4, 150.9, 130.4 (2C), 128.0, 122.0, 114.2 (2C), 102.8, 101.2, 55.4, 45.4 (2C), 45.3 (2C), 41.5. MS (ESI) *m/z*: 352 $[M+H]^+$.

*1-(4-(7H-Pyrrolo[2,3-d]pyrimidin-4-yl)piperazin-1-yl)-2-(2,4-dichlorophenyl)ethanone (**5h**)*

White solid, yield 84%, purity 97.0%, mp: 162–165°C, ^{1}H NMR (400 MHz, DMSO) δ (ppm): 11.73 (s, 1H), 8.17 (s, 1H), 7.59 (s, 1H), 7.37 (s, 2H), 7.21 (s, 1H), 6.64 (s, 1H), 3.97 (s, 2H), 3.88 (s, 4H), 3.74 (s, 2H), 3.65 (s, 2H). ^{13}C NMR (100 MHz, DMSO) δ (ppm): 168.0, 156.8, 152.4, 151.0, 135.2, 134.1, 133.7, 132.4, 128.8, 127.5, 122.0, 102.8, 101.3, 45.3 (2C), 45.2 (2C), 41.6. MS (ESI) *m/z*: 390 $[M+H]^+$.

*1-(4-(7H-Pyrrolo[2,3-d]pyrimidin-4-yl)piperazin-1-yl)-2-(naphthalen-2-yl)ethanone (**5i**)*

White solid, yield 83%, purity 98.4%, mp: 219–221°C, ^{1}H NMR (400 MHz, DMSO) δ (ppm): 11.66 (s, 1H), 8.15 (s, 1H), 7.87–7.85 (m, 3H), 7.76 (s, 1H), 7.48 (d, J = 3.5 Hz, 2H), 7.42 (d, J = 8.4 Hz, 1H), 7.18 (s, 1H), 6.60 (s, 1H), 3.95 (s, 2H), 3.87 (s, 4H), 3.70 (d, J = 18.4 Hz, 4H). ^{13}C NMR (100 MHz, DMSO) δ (ppm): 169.6, 156.8, 152.4, 150.9, 134.0, 133.5, 132.2, 128.2, 128.1, 127.9, 127.8, 127.7, 126.5, 126.0, 122.0, 102.8, 101.2, 45.5 (2C), 45.3 (2C), 41.5. MS (ESI) *m/z*: 372 $[M+H]^+$.

*1-(4-(7H-Pyrrolo[2,3-d]pyrimidin-4-yl)piperazin-1-yl)-2-(naphthalen-1-yl)ethanone (**5j**)*
White solid, yield 88%, purity 97.7%, mp: 205–208°C, ^{1}H NMR (400 MHz, DMSO) δ (ppm): 11.67 (s, 1H), 8.17 (s, 1H), 7.99 (d, J = 6.8 Hz, 1H), 7.92 (d, J = 8.8 Hz, 1H), 7.82 (d, J = 8.1 Hz, 1H), 7.57–7.42 (m, 3H), 7.37 (d, J = 6.7 Hz, 1H), 7.19 (s, 1H), 6.62 (s, 1H), 4.22 (s, 2H), 3.93 (s, 4H), 3.73 (d, J = 36.1 Hz, 4H). ^{13}C NMR (100 MHz, DMSO) δ (ppm): 169.6, 156.8, 152.4, 151.0, 133.8, 133.0, 132.6, 128.8, 127.6, 127.5, 126.4, 126.1, 125.9, 124.8, 122.0, 102.8, 101.3, 45.4 (2C), 45.3 (2C), 41.5. MS (ESI) *m/z*: 372 $[M+H]^+$.

*2-(3-Bromophenyl)-1-(4-(5-chloro-7H-pyrrolo[2,3-d]-pyrimidin-4-yl)piperazin-1-yl)ethanone (**5k**)*
White solid, yield 86%, purity 97.5%, mp: 194–196°C, ^{1}H NMR (400 MHz, DMSO) δ (ppm): 12.24 (s, 1H), 8.30 (s, 1H), 7.54 (s, 1H), 7.47–7.43 (m, 2H), 7.28–7.26 (m, 2H), 3.81 (s, 2H), 3.69 (d, J = 24 Hz, 4H), 3.55 (s, 4H). ^{13}C NMR (100 MHz, DMSO) δ (ppm): 169.1, 159.1, 151.5, 151.2, 139.2, 132.5, 130.7, 129.6, 128.8, 121.9, 121.8, 103.3, 101.6, 49.8 (2C), 49.5 (2C), 41.6. MS (ESI) *m/z*: 434 $[M+H]^+$.

*2-(4-Bromophenyl)-1-(4-(5-chloro-7H-pyrrolo[2,3-d]-pyrimidin-4-yl)piperazin-1-yl)ethanone (**5l**)*
White solid, yield 82%, purity 98.1%, mp: 189–191°C, ^{1}H NMR (400 MHz, DMSO) δ (ppm): 12.24 (s, 1H), 8.30 (s, 1H), 7.53 (s, 1H), 7.50 (d, J = 8.4 Hz, 2H), 7.21 (d, J = 8.4 Hz, 2H), 3.77 (s, 2H), 3.68 (d, J = 16.0 Hz, 4H), 3.53 (s, 4H). ^{13}C NMR (100 MHz, DMSO) δ (ppm): 169.2, 159.1, 151.5, 151.2, 135.8, 131.9 (2C), 131.5 (2C), 121.9, 119.9, 103.3, 101.6, 49.8 (2C), 49.5 (2C), 41.6. MS (ESI) *m/z*: 434 $[M+H]^+$.

*1-(4-(5-Chloro-7H-pyrrolo[2,3-d]pyrimidin-4-yl)piperazin-1-yl)-2-(naphthalen-2-yl)ethanone (**5m**)*
Pale yellow solid, yield 79%, purity 97.0%, mp: 150–153°C, ^{1}H NMR (400 MHz, DMSO) δ (ppm): 12.15 (s, 1H), 8.27 (s, 1H), 7.87 (t, J = 7.9 Hz, 3H), 7.76 (s, 1H), 7.50–7.46 (m, 3H), 7.42 (dd, J_1 = 8.5 Hz, J_2 = 1.5 Hz, 1H), 3.96 (s, 2H), 3.73 (d, J = 18.6 Hz, 4H), 3.54 (d, J = 17.8 Hz, 4H). ^{13}C NMR (100 MHz, DMSO) δ (ppm): 169.6, 159.1, 151.5, 151.2, 134.0, 133.5, 132.2, 128.2, 128.1, 127.9, 127.9, 127.7, 126.5, 126.0, 121.9, 103.3, 101.6, 49.8 (2C), 49.6 (2C), 41.6. MS (ESI) *m/z*: 406 $[M+H]^+$.

*1-(4-(5-Bromo-7H-pyrrolo[2,3-d]pyrimidin-4-yl)piperazin-1-yl)-2-phenylethanone (**5n**)*
Pale yellow solid, yield 81%, purity 98.4%, mp: 120–124°C, ^{1}H NMR (400 MHz, DMSO) δ (ppm): 12.33 (s, 1H), 8.31 (s, 1H), 7.58 (s, 1H), 7.34–7.23 (m, 5H), 3.78 (s, 2H), 3.70 (s, 4H), 3.46 (d, J = 20 Hz, 4H). ^{13}C NMR (100 MHz, DMSO) δ (ppm): 169.6, 159.6, 152.1, 151.1, 136.3, 129.4 (2C), 128.8 (2C), 126.8, 124.8, 104.9, 86.3, 50.3 (2C), 50.2 (2C), 41.5. MS (ESI) *m/z*: 400 $[M+H]^+$.

*1-(4-(5-Bromo-7H-pyrrolo[2,3-d]pyrimidin-4-yl)piperazin-1-yl)-2-(3-bromophenyl)ethanone (**5o**)*
Pale white solid, yield 83%, purity 97.8%, mp: 184–186°C, ^{1}H NMR (400 MHz, DMSO) δ (ppm): 12.33 (s, 1H), 8.32 (s, 1H), 7.59 (s, 1H), 7.47–7.43 (m, 2H), 7.30–7.26 (m, 2H), 3.81 (s, 2H), 3.71 (d, J = 16 Hz, 4H), 3.50 (s, 4H). ^{13}C NMR (100 MHz, DMSO) δ (ppm): 169.1, 159.6, 152.1, 151.1, 139.2, 132.5, 130.7, 129.7, 128.8, 124.8, 121.8, 104.9, 86.3, 50.4 (2C), 50.2 (2C), 41.6. MS (ESI) *m/z*: 480 $[M+H]^+$.

*1-(4-(5-Bromo-7H-pyrrolo[2,3-d]pyrimidin-4-yl)piperazin-1-yl)-2-(4-bromophenyl)ethanone (**5p**)*
Pale yellow solid, yield 89%, purity 98.1%, mp: 176–178°C, ^{1}H NMR (400 MHz, DMSO) δ (ppm): 12.31 (s, 1H), 8.31 (s, 1H), 7.58 (s, 1H), 7.50 (d, J = 8.4 Hz, 2H), 7.21 (d, J = 8.4 Hz, 2H), 3.77 (s, 2H), 3.70 (t, J = 6.28 Hz, 4H), 3.48 (d, J = 3.36 Hz, 4H). ^{13}C NMR (100 MHz, DMSO) δ (ppm): 169.2, 159.6, 152.1, 151.1, 135.8, 131.9 (2C), 131.5 (2C), 124.8, 119.9, 104.9, 86.2, 50.4 (4C), 50.2 (4C), 41.6. MS (ESI) *m/z*: 480 $[M+H]^+$.

*1-(4-(5-Bromo-7H-pyrrolo[2,3-d]pyrimidin-4-yl)piperazin-1-yl)-2-(4-chlorophenyl)ethanone (**5q**)*
Pale yellow solid, yield 70%, purity 97.9%, mp: 193–195°C, ^{1}H NMR (400 MHz, DMSO) δ (ppm): 12.32 (s, 1H), 8.31 (s, 1H), 7.59 (s, 1H), 7.37 (d, J = 8.4 Hz, 2H), 7.27 (d, J = 8.4 Hz, 2H), 3.79 (s, 2H), 3.76–3.65 (m, 4H), 3.49 (d, J = 3.5 Hz, 4H). ^{13}C NMR (100 MHz, DMSO) δ (ppm): 169.2, 156.8, 152.4, 150.9, 135.8, 132.0 (2C), 131.5 (2C), 129.1, 122.0, 119.9, 102.8, 101.2, 45.3 (4C), 41.5. MS (ESI) *m/z*: 434 $[M+H]^+$.

*1-(4-(5-Bromo-7H-pyrrolo[2,3-d]pyrimidin-4-yl)piperazin-1-yl)-2-(4-methoxyphenyl)ethanone (**5r**)*
Pale yellow solid, yield 88%, purity 98.5%, mp: 170–173°C, ^{1}H NMR (400 MHz, DMSO) δ (ppm): 12.33 (s, 1H), 8.30 (s, 1H), 7.58 (s, 1H), 7.17 (d, J = 8.0 Hz, 2H), 6.88 (d, J = 8.0 Hz, 2H), 3.73–3.70 (m, 9H), 3.45 (d, J = 20 Hz, 4H). ^{13}C NMR (100 MHz, DMSO) δ (ppm): 169.9, 159.6, 158.3, 152.1, 151.1, 130.4 (2C), 128.0, 124.8, 114.2 (2C), 104.9, 86.3, 55.4, 50.3 (2C), 50.3 (2C), 41.5. MS (ESI) *m/z*: 430 $[M+H]^+$.

*1-(4-(5-Bromo-7H-pyrrolo[2,3-d]pyrimidin-4-yl)piperazin-1-yl)-2-(4-(tert-butyl)phenyl)ethanone (**5s**)*
Pale yellow solid, yield 85%, purity 99.2%, mp: 113–116°C, ^{1}H NMR (400 MHz, DMSO) δ (ppm): 12.24 (s, 1H), 8.29 (s, 1H), 7.53 (s, 1H), 7.33 (d, J = 8.0 Hz, 2H), 7.17 (d, J = 8.0 Hz, 2H), 3.73 (s, 2H), 3.68 (s, 4H), 3.52 (d, J = 12 Hz, 4H), 1.27 (s, 9H). ^{13}C NMR (100 MHz, DMSO) δ (ppm): 169.7, 159.1, 151.2, 149.0, 133.2, 129.4, 129.1, 125.5, 121.9, 103.2, 101.6, 49.8 (2C), 49.5 (2C), 41.5, 34.5, 31.6 (3C). MS (ESI) *m/z*: 456 $[M+H]^+$.

*1-(4-(5-Bromo-7H-pyrrolo[2,3-d]pyrimidin-4-yl)piperazin-1-yl)-2-(3,4-dichlorophenyl)ethanone (**5t**)*
Yellow solid, yield 78%, purity 97.7%, mp: 149–152°C, ^{1}H NMR (400 MHz, DMSO) δ (ppm): 12.34 (s, 1H), 8.32 (s, 1H), 7.59–7.53 (m, 3H), 7.24 (d, J = 8.4 Hz, 1H), 3.83 (s, 2H), 3.71 (d, J = 20 Hz, 4H), 3.52 (s, 4H). ^{13}C NMR (100 MHz, DMSO) δ (ppm): 169.9, 158.3, 156.8, 152.4, 150.9, 130.4 (2C), 128.0, 122.0, 114.2 (2C), 102.8, 101.2, 55.4, 45.4 (2C), 45.3 (2C), 41.5. MS (ESI) *m/z*: 468 $[M+H]^+$.

*1-(4-(5-Bromo-7H-pyrrolo[2,3-d]pyrimidin-4-yl)piperazin-1-yl)-2-(naphthalen-2-yl)ethanone (**5u**)*
Pale yellow solid, yield 80%, purity 98.3%, mp: 144–146°C, ^{1}H NMR (400 MHz, DMSO) δ (ppm): 12.25 (s, 1H), 8.29 (s, 1H), 7.87 (t, $J = 7.8$ Hz, 3H), 7.77 (s, 1H), 7.55 (s, 1H), 7.52–7.44 (m, 2H), 7.42 (dd, $J_1 = 8.4$ Hz, $J_2 = 1.6$ Hz, 1H), 3.96 (s, 2H), 3.75 (d, $J = 16.0$ Hz, 4H), 3.49 (d, $J = 19.7$ Hz, 4H). ^{13}C NMR (100 MHz, DMSO) δ (ppm): 169.5, 159.6, 152.1, 151.1, 134.0, 133.5, 132.2, 128.2, 128.1, 128.0, 127.9, 127.7, 126.5, 126.0, 124.8, 104.9, 86.3, 50.4 (2C), 50.3 (2C), 41.6. MS (ESI) *m/z*: 450 $[M+H]^+$.

Biology

In vitro Akt1 kinase activity assay
In vitro Akt1 kinase activity was evaluated in 384-well plates using the HTRF assay (LANCE®), which has been well validated and applied to a number of enzymatic activity assays [11]. The assay format involves two steps. Kinase reaction step: each well was added Akt1 (0.075 ng/μL), STK Substrate-biotin (0.25 μM), gradient-diluted compound (0.064–5000 nM) in kinase buffer (50 mM HEPES, 5 mM $MgCl_2$, 1 mM DTT, 0.02% NaN_3, and 0.01% BSA, pH = 7.0), then ATP (13.42 μM) in kinase buffer was added to start the reaction, the plate was incubated for 45 min at 37°C. During this step, only the active kinase phosphorylated the substrate. Detection step: Sa-XL665 conjugate (0.0625 μM) and STK Ab-Cryptate (5 μL) were added to the wells and incubated for 2 h. During this step, EDTA in the detection buffer stopped the enzymatic reaction, the detection reagents caught the phosphorylated substrate. Then the fluorescence was measured at 620 and 665 nm using a microplate reader (PerkinElmer, USA). The resulting HTRF signal, ratio = $(EM_{665}/EM_{620}) \times 10^4$, was proportional to the phosphorylation level, which reflected the inhibitory level of Akt1 enzyme.

MTT assay
The antiproliferative effects of the target compounds on the LNCaP and PC-3 cell lines were tested using the MTT assay. The cells were seeded in 96-well microplates at a density of 5×10^3 cells per well and cultured in a humidified atmosphere with 5% CO_2 at 37°C. When attached to the bottom, the cells were treated with compounds at final concentrations ranging from 5 to 80 μM for PC-3 cells (2.5–40 μM LNCaP cells). The final concentration of DMSO in medium was less than 0.5%. After 72 h of incubation, 5 mg/mL MTT (10 μL) was added followed by another 4 h incubation, then the supernatant was removed and the formazan crystal was extracted by DMSO. The optical density ($OD_{570\,nm}$) value was detected using a microplate reader (Bio-Rad 680, USA). The IC_{50} was calculated using PRISM version 5.0 software from the non-linear curve.

Molecular docking

Molecular docking was performed using the Sybyl 1.1 program and the Akt1 crystal structure (PDB: 4EKL). Protein preparation was performed by extracting the ligand, removing water molecules, adding hydrogen atoms, and assigning AMBER7 FF99 charges to the protein. All of the target compounds were docked into Akt1 and formed hydrogen bonds and hydrophobic interactions in the model. After docking calculations, 20 binding poses per ligand were generated, and the best conformation with the highest CScore was selected for subsequent interaction analysis.

This work was supported by the National Natural Science Foundation of China (no. 21272140) and Projects of Shandong Science and Technology (no. 2014GSF119003).

The authors have declared no conflicts of interest.

References

[1] B. D. Manning, L. C. Cantley, *Cell* **2007**, *129*, 1261–1274.
[2] E. Fayard, G. Xue, A. Parcellier, L. Bozulic, B. A. Hemmings, *Curr. Top. Microbiol. Immunol.* **2010**, *346*, 31–56.
[3] I. Hers, E. E. Vincent, J. M. Tavare, *Cell. Signal.* **2011**, *23*, 1515–1527.
[4] J. Q. Cheng, C. W. Lindsley, G. Z. Cheng, H. Yang, S. V. Nicosia, *Oncogene* **2005**, *24*, 7482–7492.
[5] D. Yang, P. Wang, J. Liu, H. Xing, Y. Liu, W. Xie, G. Zhao, *Bioorg. Med. Chem.* **2014**, *22*, 366–373.
[6] E. Paplomata, R. O'Regan, *Ther. Adv. Med. Oncol.* **2014**, *6*, 154–166.
[7] C. De Marco, N. Rinaldo, P. Bruni, C. Malzoni, F. Zullo, F. Fabiani, S. Losito, M. Scrima, F. Z. Marino, R. Franco, A. Quintiero, V. Agosti, G. Viglietto, *PLoS ONE* **2013**, *8*, e55362.
[8] M. P. Edlind, A. C. Hsieh, *Asian J. Androl.* **2014**, *16*, 378–386.
[9] J. A. McCubrey, M. L. Sokolosky, B. D. Lehmann, J. R. Taylor, P. M. Navolanic, W. H. Chappell, S. L. Abrams, K. M. Stadelman, E. W. Wong, N. Misaghian, S. Horn, J. Basecke, M. Libra, F. Stivala, G. Ligresti, A. Tafuri, M. Milella, M. Zarzycki, A. Dzugaj, F. Chiarini, C. Evangelisti, A. M. Martelli, D. M. Terrian, R. A. Franklin, L. S. Steelman, *Adv. Enzyme Regul.* **2008**, *48*, 113–135.
[10] P. Wang, L. Zhang, Q. Hao, G. Zhao, *Mini. Rev. Med. Chem.* **2011**, *11*, 1093–1107.
[11] F. Degorce, A. Card, S. Soh, E. Trinquet, G. P. Knapik, B. Xie, *Curr. Chem. Genomics* **2009**, *28*, 22–32.